Synchrotron x-ray-diffraction study of orbital ordering in YVO_3

M. Noguchi,[1] A. Nakazawa,[1] S. Oka,[1] T. Arima,[1] Y. Wakabayashi,[2] H. Nakao,[2] and Y. Murakami[2,3]

[1]*Institute of Materials Science, University of Tsukuba, Tsukuba 305-8573, Japan*

[2]*Photon Factory, Institute of Materials Structure Science, High Energy Accelerator Research Organization, Tsukuba 305-0801, Japan*

[3]*Core Research for Evolutional Science and Technology (CREST), Tsukuba 305-0047, Japan*

(Received 28 April 2000)

Synchrotron x-ray-diffraction experiments have been carried out in a perovskite-type vanadium oxide YVO_3 to elucidate orbital ordering of the system. The change from *C*- to *G*-type orbital ordering at the lower magnetic transition temperature was strongly suggested. The long-range orbital ordering appears also in the high-temperature paramagnetic phase. Azimuthal-angle dependence of orbital superlattice reflections indicates that for both orbital-ordering phases the orbital occupation is approximately the $d^1_{xy}d^1_{yz}$ and $d^1_{xy}d^1_{zx}$ configuration in two sublattices, respectively. These results are in good agreement with a theoretical prediction.

Recently, Ren *et al.* found temperature-induced magnetization reversals in YVO_3.[1] The perovskitelike vanadium oxide compound is a Mott insulator[2] and has a *Pbnm* orthorhombic unit cell with $a \sim b \sim \sqrt{2}a_p$ and $c \sim 2a_p$ (a_p being the lattice parameter of cubic perovskite).[3] A neutron-scattering study reveals that YVO_3 has two magnetic ordering phases.[4] Below the first Néel temperature $T_{N1}=118$ K, the magnetic structure is antiferromagnetic in the ab plane and ferromagnetic along the c axis (so-called *C* type). In the low-temperature phase below $T_{N2} \sim 77$ K, however, the V^{3+} spins are antiferromagnetically arranged both in the ab plane and along the c axis (so-called *G*-type magnetic structure). The change in magnetic structure should be caused by a sign change in the superexchange interaction between neighboring V^{3+} ions along the c axis. It is well established that such a sign change can be set for different orbital occupations in an orbitally ordered material.[5–7] In fact, a structural study strongly suggested orbital ordering in the low-temperature phase.[4] The magnetic transition at T_{N2} is accompanied by a distortion of VO_6 octahedra. All the VO_6 octahedra are elongated alternately along the x or y axis in the low-temperature phase, while two kinds of V–O bonds in the ab plane are almost equal in length above T_{N2}. Here the local coordination axes x, y, and z are along the V–O bond directions near [110], $[\bar{1}10]$, and [001], respectively. Taking into account the Jahn-Teller (JT) effect of V^{3+} with two t_{2g} electrons, the d_{zx} and d_{yz} orbitals should be occupied by turns as shown in Fig. 1(a). By analogy with magnetic structure, we call the orbital ordering *C* type. The *C*-type orbital ordering was also obtained by a local density approximation+U band calculation.[8]

Another type of orbital ordering has been predicted in the intermediate-temperature phase of YVO_3.[9,10] The possible orbital ordering is schematically drawn in Fig. 1(b). However, the orbital state above T_{N2} is not so clear as in the low-temperature phase, because VO_6 octahedra are little distorted. It is also suggested that the above-mentioned multiple magnetic reversals should be closely related to orbital ordering in YVO_3. The magnetic easy axis at each V^{3+} site should be governed by the *d*-orbital occupation through spin-orbit coupling. Temperature-dependent occupation of the *d* orbitals can alter the canting angle in the weak ferromagnet YVO_3 and hence cause the magnetic reversals.

In this paper we present synchrotron x-ray-scattering experiments in YVO_3 around the *K* edge of vanadium that demonstrate a change in orbital ordering at T_{N2}. Resonant x-ray diffraction is sensitive to the occupancy of V $3d$ orbitals

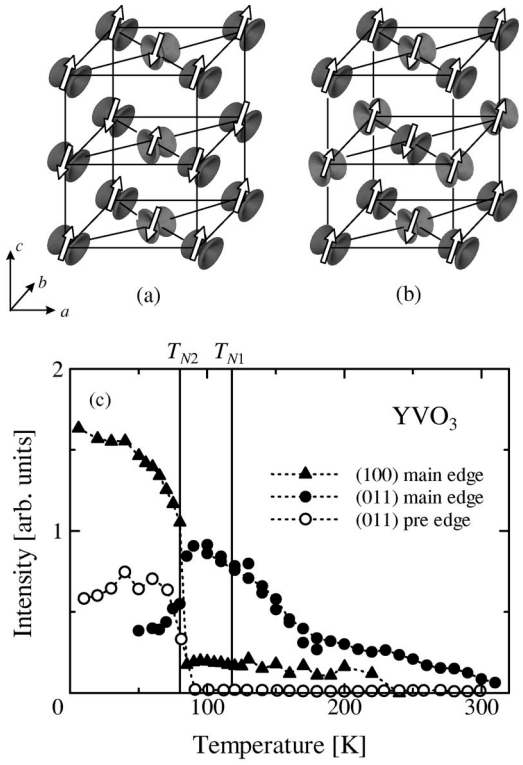

FIG. 1. The predicted ordering of spin (arrows) and orbital degrees of freedom in YVO_3. The orientation of arrows does not display the real spin axis: (a) *G*-type AFM spin ordering with *C*-type orbital ordering in the low-temperature phase and (b) *C*-type AFM spin ordering with *G*-type orbital ordering in the intermediate-temperature phase. (c) Closed triangles and circles: Integrated intensity of x-ray (100) and (011) reflections at the vanadium *K* main edge as a function of temperature. Open circles: The (011) reflection at the pre-edge as a function of temperature. The incident beam is polarized perpendicular to the c axis.

because it probes the split of unoccupied V $4p$ states caused by the $3d$-$4p$ Coulomb interaction or the ligand field effect.[11–13] Though it has not been settled whether the orbital ordering or the cooperative Jahn-Teller distortion dominates the resonant scattering, it has been reported that the (030) orbital scattering at the Mn K edge in $La_{1-x}Sr_xMnO_3$ with $x=0.12$ was observed below $T_{OO}=145$ K, while the large cooperative elongation of MnO_6 octahedra was observed above T_{OO}.[14,15] Therefore, we consider the resonant x-ray-diffraction technique to be a powerful tool to investigate orbital ordering. In addition, one can obtain important information about the orbital symmetries at each sublattices by investigating dependence of orbital-ordering diffraction on the direction of the electric field of the incident beam.

A single-domain crystal boule of YVO_3 with a diameter of 4 mm was grown by a floating-zone technique. Two samples were prepared for the present x-ray study: one was cut to form a (100) surface and the other (011). Resonant x-ray-diffraction experiments were performed at the beamline 4C of the Photon Factory, Japan. We have tuned the incident energy near the V^{3+} K edge by double Si(111) crystals. The typical energy resolution was 2 eV. The beam with the electric field perpendicular to the scattering plane (σ polarization) was focused on a sample by a bent cylindrical mirror. The sample was mounted in a closed-cycle He refrigerator on a four-axis diffractometer. In order to analyze whether the polarization of the scattered beam is parallel (π' polarization) or perpendicular (σ' polarization) to the scattering plane, we used a pyrolitic graphite (0004) crystal, which gives a scattering angle of 85.1°.

Figure 2(a) shows the absorption spectrum of YVO_3. The rising of the absorption spectrum near 5.48 keV is due to the V^{3+} K main edge, which corresponds to the threshold energy of the $1s$-$4p$ intra-atomic dipole transition. The pre-edge ($1s$-$3d$ threshold energy) appears as a small peak at 5.466 keV. Figures 2(b) and 2(c) show dependence of the intensity of the (100) and (011) reflections on x-ray photon energy. These reflections do not obey the extinction rule and correspond to the propagation vectors for C- and G-type ordering, respectively. We found that the (100) reflection was π' polarized, while the (011) reflection contained both polarization components with the nearly same photon-energy dependence. Both reflections show the resonance around the V^{3+} K main edge and almost disappear for photon energies well below the K edge. It is noteworthy that the π' polarization and the complicated resonance effect can be explained neither by multiple scattering nor by lattice distortion. The strong resonance manifests a modulation of the electronic state of V^{3+} ions. At the pre-edge much less resonance is observed than in the case of V_2O_3,[16] on account of the inversion symmetry at the V site in YVO_3. For the (100) orbital reflection other strong resonance peaks can be observed above the K main edge. The intensity at 5.495 keV shows almost the same temperature dependence as at the main edge. By contrast, the (100) reflection at 5.487 keV even intensifies in the intermediate-temperature phase. Such multiple strong resonance of orbital reflections has been reported neither in manganese oxide compounds nor in V_2O_3.[11,16–20] Further theoretical work taking into account a similar mechanism as the extended x-ray absorption fine structure is needed to understand the origin of these resonance peaks.

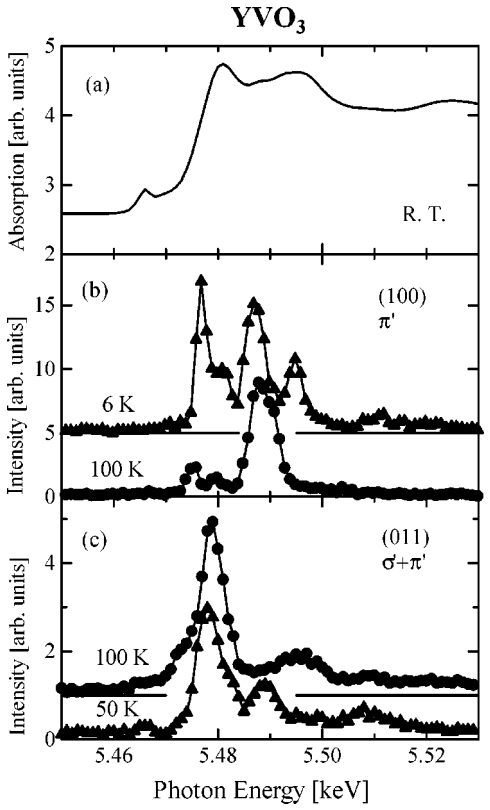

FIG. 2. (a) Absorption spectrum of YVO_3 powder at room temperature. (b) Photon-energy dependence of intensity of the π' component of the (100) orbital reflection at 6 and 100 K. Measurements were performed with the $\vec{E}_i \| b$ configuration. (c) Photon-energy dependence of intensity of the (011) orbital reflection measured with the $\vec{E}_i \| c$ configuration at 50 and 100 K.

Temperature dependence of the integrated intensity of the superlattice scattering at the main edge in a warming run is displayed in Fig. 1(c). Here the (011) intensity at the pre-edge is also plotted. The (100) reflection at the main edge suddenly reduces intensity as increasing temperature beyond T_{N2}. On the contrary, the (011) reflection at the main edge becomes stronger with a small jump as heating beyond T_{N2}. The (011) reflection below T_{N2} might be due to the C-type orbital ordering in the distorted perovskite structure as indicated by azimuthal-angle dependence (see below). The temperature dependence of the x-ray reflections around T_{N2} is opposite of that of neutron magnetic scattering with the same indices.[4] The (011) reflection at the pre-edge is similar in temperature dependence to the (100) reflection at the main edge. Further theoretical studies are necessary to interpret the present data. The mechanism of the x-ray resonant reflection at the $1s$-$3d$ absorption edge is not clear yet except for the cases with no inversion symmetry.[21] The process of the pre-edge resonance would possibly be enhanced by the elongation of the VO_6 octahedra.

The results of the resonant scattering at the main edge strongly demonstrate a change in orbital ordering from C type to G type at T_{N2} in the manner of a first-order transition. The C-type orbital ordering in the low-temperature phase corresponds well to the cooperative distortion of VO_6 octahedra below T_{N2}. In opposition, the G-type orbital ordering is not associated with Jahn-Teller distortion, because it

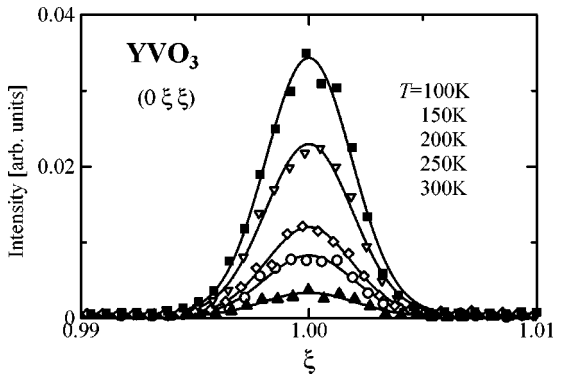

FIG. 3. Peak profiles of the (011) resonant orbital scattering with a 2θ-ω scan at various temperatures.

would violate the mirror symmetry normal to the *c* axis of a *Pbnm* lattice system. The (011) intensity reaches a maximum at around 100 K and then gradually decreases with a small kink at around 180 K. One cannot see any anomaly at T_{N1}. The *G*-type orbital ordering appears not only in the intermediate-temperature *C*-type antiferromagnetic (AFM) phase but also in the high-temperature paramagnetic phase. Figure 3 shows the (011) peak profiles with a $(0\xi\xi)$ scan at various temperatures. The measurement was performed with a resolution of $\Delta\xi\sim 0.003$. The peak has a nearly temperature-independent full width at half maximum of about 0.004. The orbital ordering exhibits a long-range nature with a correlation length of $\geqslant 10^3$ Å .

A possible scenario of the successive phase transitions in the spin-orbital-correlated vanadate system is the following. In cooling from room temperature the *G*-type orbital ordering first grows. Then the *C*-type AFM phase originates from anisotropic superexchange interaction on account of the orbital ordering.[7] With further decreasing temperature, the orbital ordering would cause the cooperative lattice distortion.

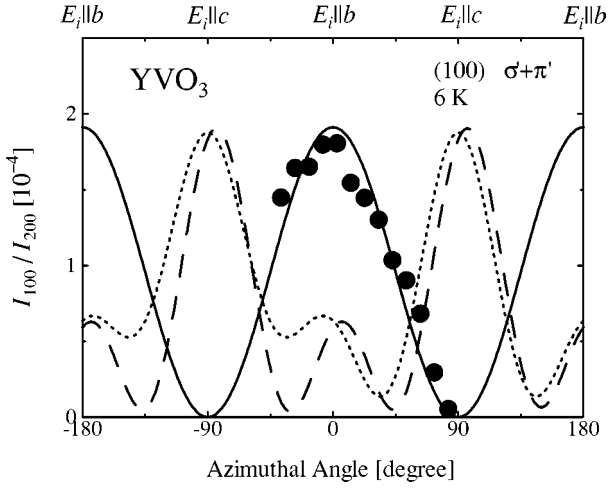

FIG. 4. Circles: intensity of the (100) orbital reflection normalized by the (200) fundamental reflection as a function of azimuthal angle Ψ. $\Psi=0$ denotes the configuration of $\vec{E}_i\|b$. The measurements were performed at 6 K using the x-ray beam with a photon energy of the V^{3+} *K* main edge. Lines show calculations for *C*-type ordering of the following orbital symmetries: $d_{xy}d_{zx}/d_{xy}d_{yz}$ (solid line), $d_{xy}d_{zx}/d_{zx}d_{yz}$ (dotted line), and $d_{xy}d_{yz}/d_{zx}d_{yz}$ (long-dashed line).

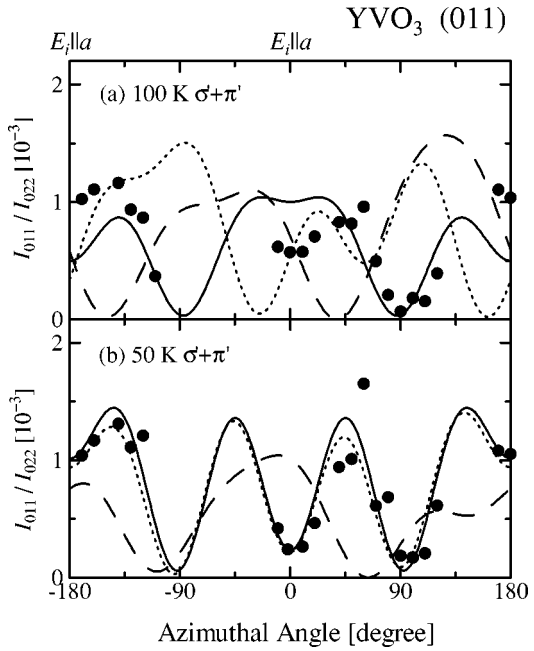

FIG. 5. Circles: intensity of the (011) orbital reflection normalized by the (022) fundamental reflection as a function of azimuthal angle Ψ, at (a) 100 K and (b) 50 K. $\Psi=0$ denotes the configuration of $\vec{E}_i\|a$. The measurements were performed using the x-ray beam with a photon energy of the V^{3+} *K* main edge. Lines show calculations for (a) *G*- and (b) *C*-type ordering of the following orbital symmetries: $d_{xy}d_{zx}/d_{xy}d_{yz}$ (solid line), $d_{xy}d_{zx}/d_{zx}d_{yz}$ (dotted line), and $d_{xy}d_{yz}/d_{zx}d_{yz}$ (long-dashed line).

However, as Mizokawa *et al.* have pointed out, the energy gain by the JT distortion in the *G*-type orbital ordering state is less than in the *C*-type orbital ordering state, considering the tilting and rotating of VO_6 octahedra.[10] As a result, the compound changes from the *C*-type AFM state with *G*-type orbital ordering to the *G*-type AFM state with *C*-type orbital ordering and cooperative JT distortion.

Since the synchrotron radiation is linearly polarized, the azimuthal angle Ψ, denoting the rotation of a sample around the scattering vector, determines the direction of the electric vector of the incident beam, $\vec{E}_i$, in the crystallographic coordinates. The symmetry of the vanadium degenerate orbital states at each sublattice can be investigated through Ψ dependence of orbital reflections. As shown in Fig. 4 the (100) reflection is maximum with the $\vec{E}_i\|b$ configuration and nearly vanishes with $\vec{E}_i\|c$. Model calculations for three types of orbital symmetries at the two sublattices in *C*-type ordering are also shown in the panel: $d^1_{xy}d^1_{zx}/d^1_{xy}d^1_{yz}$ (solid line), $d^1_{xy}d^1_{zx}/d^1_{zx}d^1_{yz}$ (dotted line), and $d^1_{xy}d^1_{yz}/d^1_{zx}d^1_{yz}$ (long-dashed line). In our calculations, the atomic scattering tensor of each V^{3+} ion is assumed to be of uniaxial type on the *xyz* coordinates as in the case of Mn^{3+}.[11] For example, the anomalous scattering tensor of a V^{3+} ion with the $d^1_{xy}d^1_{yz}$ configuration is assumed to be

$$f=\begin{pmatrix} f_\perp & 0 & 0 \\ 0 & f_\parallel & 0 \\ 0 & 0 & f_\perp \end{pmatrix}. \qquad (1)$$

The experimental data are well fitted with the calculation for *C*-type ordering of the $d^1_{xy}d^1_{zx}$ and $d^1_{xy}d^1_{yz}$ configurations shown by a solid line. The orbital-ordering model agrees well with the π' polarization of the (100) reflection. The orbital model can also explain the (011) reflection below T_{N2}. The solid line in Fig. 5(b), which shows the calculation for the *C*-type orbital ordering with a rotation around the *c* axis of 15° and a tilting from the *c* axis of 18° of each VO_6 octahedron,[4] explains the general trend of the experimental data at 50 K.

Azimuthal-angle dependence of the (011) reflection at 100 K is shown in Fig. 5(a). The calculation for the *G*-type ordering of $d^1_{xy}d^1_{zx}$ and $d^1_{xy}d^1_{yz}$ configurations fits the data best among the three models shown in the panel, though the agreement is not sufficiently good. It is possible that other orbitals should be partially occupied, which modifies the symmetry axes at each V site. A magnetic reversal at around 95 K (Ref. 1) is also indicative that the orbital symmetry axes would be dependent of temperature in the intermediate-temperature phase.

In summary, we observed resonant x-ray reflections of (100) and (011) related to orbital ordering in YVO_3. The *G*-type AFM spin ordering is accompanied by *C*-type orbital ordering, and the *C*-type AFM by *G*-type orbital ordering. Azimuthal-angle dependence of the orbital reflections clearly shows that in the low-temperature phase, one electron occupies the d_{xy} orbital at every V site, and the d_{zx} or d_{yz} orbital is alternatively occupied. The result is in good agreement with a theoretical prediction. The symmetry axes of the orbital occupation would be slightly modified in the *G*-type orbital-ordering state. The long-range *G*-type orbital ordering appears not only in the intermediate-temperature *C*-type AFM phase but also in the high-temperature paramagnetic phase.

The authors would like to thank Y. Tokura for the use of a floating-zone furnace. This work was supported by the Ministry of Education, Science and Culture of Japan.

[1] Y. Ren, T. T. M. Palstra, D. I. Khomskii, E. Pellegrin, A. A. Nugroho, A. A. Menovsky, and G. A. Sawatzky, Nature (London) **396**, 441 (1998).

[2] See for example, M. Kasuya, Y. Tokura, T. Arima, H. Eisaki, and S. Uchida, Phys. Rev. B **47**, 6197 (1993); T. Arima, Y. Tokura, and J. B. Torrance, *ibid.* **48**, 17 006 (1993).

[3] D. B. Rogers, A. Ferretti, D. H. Ridgley, R. J. Arnott, and J. B. Goodenough, J. Appl. Phys. **37**, 1431 (1966); V. G. Zubkov, A. S. Borukhovich, G. V. Bazuev, K. K. Matveenko, and G. P. Shveikin, Zh. Éksp. Teor. Fiz. **66**, 1823 (1974) [Sov. Phys. JETP **39**, 896 (1974)].

[4] H. Kawano, H. Yoshizawa, and Y. Ueda, J. Phys. Soc. Jpn. **63**, 2867 (1994).

[5] J. B. Goodenough, Phys. Rev. **100**, 564 (1955).

[6] J. Kanamori, J. Phys. Chem. Solids **10**, 87 (1959).

[7] K. I. Kugel and D. I. Khomskii, Pis'ma Zh. Éksp. Teor. Fiz. **15**, 629 (1972) [JETP Lett. **15**, 446 (1972)].

[8] H. Sawada and K. Terakura, Phys. Rev. B **58**, 6831 (1998).

[9] H. Sawada, N. Hamada, K. Terakura, and T. Asada, Phys. Rev. B **53**, 12 742 (1996).

[10] T. Mizokawa, D. I. Khomskii, and G. A. Sawatzky, Phys. Rev. B **60**, 7309 (1999).

[11] Y. Murakami, H. Kawada, H. Kawata, M. Tanaka, T. Arima, Y. Moritomo, and Y. Tokura, Phys. Rev. Lett. **80**, 1932 (1998).

[12] S. Ishihara and S. Maekawa, Phys. Rev. Lett. **80**, 3799 (1998).

[13] I. S. Elfimov, V. I. Anisimov, and G. A. Sawatzky, Phys. Rev. Lett. **82**, 4264 (1999); M. Benfatto, Y. Joly, and C. R. Natoli, *ibid.* **83**, 636 (1999).

[14] Y. Endoh, K. Hirota, S. Ishihara, S. Okamoto, Y. Murakami, A. Nishizawa, T. Fukuda, H. Kimura, H. Nojiri, K. Kaneko, and S. Maekawa, Phys. Rev. Lett. **82**, 4328 (1999).

[15] B. Dabrowski, X. Xiong, Z. Bukowski, R. Dybzinski, P. W. Klamut, J. E. Siewenie, O. Chmaissem, J. Shaffer, C. W. Kimball, J. D. Jorgensen, and S. Short, Phys. Rev. B **60**, 7006 (1999).

[16] L. Paolasini, C. Vettier, F. de Bergevin, F. Yakhou, D. Mannix, A. Stunault, W. Neubeck, M. Altarelli, M. Fabrizio, P. A. Metcalf, and J. M. Honig, Phys. Rev. Lett. **82**, 4719 (1999).

[17] Y. Murakami, J. P. Hill, D. Gibbs, M. Blume, I. Koyama, M. Tanaka, H. Kawata, T. Arima, Y. Tokura, K. Hirota, and Y. Endoh, Phys. Rev. Lett. **81**, 582 (1998).

[18] Y. Endoh, K. Hirota, S. Ishihara, S. Okamoto, Y. Murakami, A. Nishizawa, T. Fukuda, H. Kimura, H. Nojiri, K. Kaneko, and S. Maekawa, Phys. Rev. Lett. **82**, 4328 (1999).

[19] M. v. Zimmermann, J. P. Hill, D. Gibbs, M. Blume, D. Casa, B. Keimer, Y. Murakami, Y. Tomioka, and Y. Tokura, Phys. Rev. Lett. **83**, 4872 (1999).

[20] K. Nakamura, T. Arima, A. Nakazawa, Y. Wakabayashi, and Y. Murakami, Phys. Rev. B **60**, 2425 (1999).

[21] In the case with no inversion symmetry, a dipole component is considered to be dominant. See M. Fabrizio, M. Altarelli, and M. Benfatto, Phys. Rev. Lett. **80**, 3400 (1998).